[Geophysical Research Letters]

Supporting Information for

Electrostatic waves around a magnetopause reconnection diffusion region and their associations with whistler and lower-hybrid waves

Shan Wang[1*], Daniel B. Graham[2], Xin An[3], Li Li[1], Qiu-Gang Zong[1], Xu-Zhi Zhou[1], Wen-Ya Li[4], and Zhi-Yang Liu[1]

[1]Institute of Space Physics and Applied Technology, Peking University, Beijing, China 100871

[2]Swedish Institute of Space Physics, Uppsala SE-75121, Sweden

[3]Department of Earth, Planetary, and Space Sciences, University of California, Los Angeles, California, USA, 90095

[1]State Key Laboratory of Space Weather, National Space Science Center, Chinese Academy of Sciences, Beijing, China, 100190

Contents of this file

Introduction

This supplementary information provides descriptions of satellite data used in the analysis, and details about how we model the observed non-gyrotropic distribution shown in Figure 2.

Text S1

Data are from the Magnetospheric Multiscale (MMS) mission burst-mode measurements. The magnetic fields are from the Flux Gate Magnetometer at 128 samples/s (Russell et al., 2016) and Search Coil Magnetometer at 8,192 samples/s (Le Contel, Leroy, Roux et al.,

2016). Electric fields are from the double probes at 8,192 samples/s (Ergun et al., 2016; Lindquvist et al., 2016; Torbert et al., 2016), where the DC-coupled 'dce' product has 8,192 samples/s and the AC-coupled 'hmfe' product that have fewer available intervals than 'dce' data has 65,536 samples/s. Plasma data are from the Fast Plasma Investigation (Pollock et al., 2016), where the ion and electron measurements have time resolutions of 0.15 s and 0.03 s, respectively.

Text S2

We use 5 populations to model the distribution by finding the optimal fitting result. The corresponding velocity ranges are marked in the observed distribution sliced in the vpara-vperp1 plane at vperp2=0 (Figure S1a). Brief explanations for the populations are written on its right. Figures S1b-S1d show the fitting for population 1. The black boxes mark the velocity range used for fitting, and panel d shows 1D cuts along velocities marked in 2D panels, with reasonable agreements. The parameters are written on the right. Similarly, Figures S1e-S1g show the fitting result for population 2. Note that the modeled distribution extends to a larger velocity range than that used for fitting.

Figure S2 shows the modeling procedure for populations 3-5 that represent the non-gyrotropic beam, with similar formats as in Figure S1. We first subtract the original observed distribution by the model populations 1 and 2 and then fit the remaining distribution. The 1D comparisons again show reasonable agreements between the observation and model distributions.

Figure S3 shows the comparison between the observed distribution with the model distribution that sums over all 5 populations. Two sets of 1D cuts are provided for comparison. The model distribution captures the main features of the observed distribution, though quantitative discrepancies exist.

When applying in the linear instability analysis, ions are set to have a density of 11.7 cm^{-3} to keep the charge neutrality with the model electron distribution, slightly smaller than the observed level of 14.7 cm^{-3}. The ion temperatures are T_{ipara}=650 eV, T_{iperp}=527 eV. The observed ion bulk velocities are V_{ipara}=75 km/s, V_{iperp1}=-25 km/s, and V_{iperp2}=-25 km/s, which are neglected in the instability analysis.

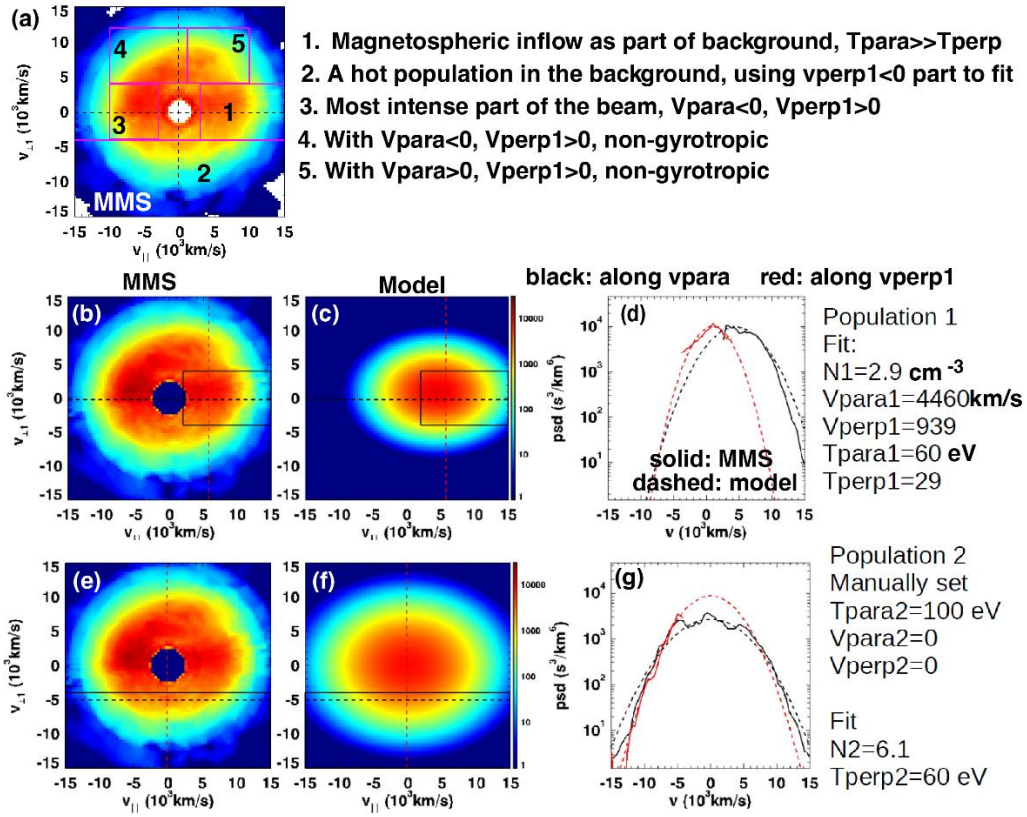

Figure S1. Observed and model distribution for background populations

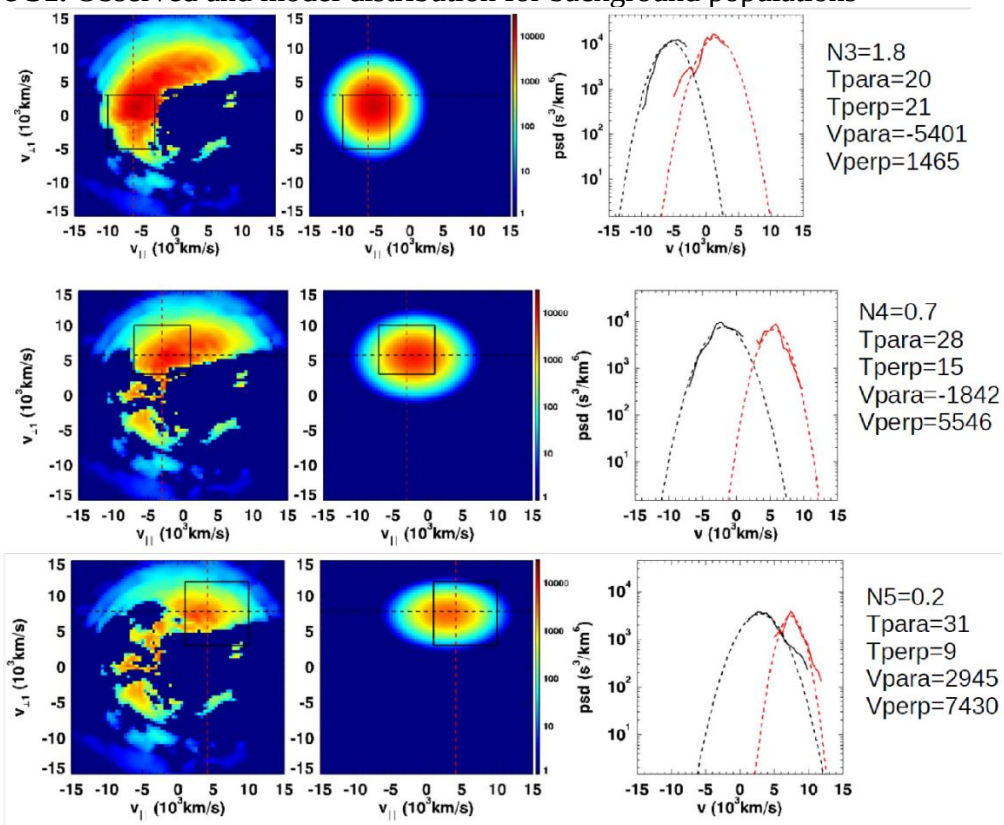

Figure S2. Observed and model distributions for the non-gyrotropic beam

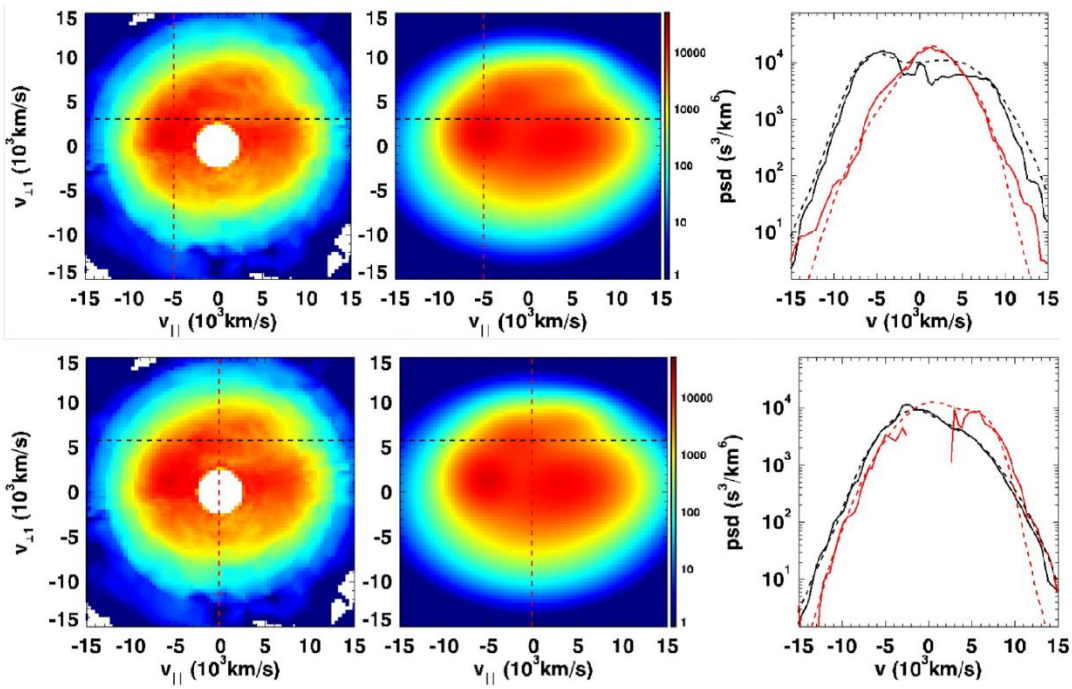

Figure S3. Observed and model distributions that sum up all populations.

References

Ergun, R., Tucker, S., Westfall, J., Goodrich, K., Malaspina, D., & Summers, D. (2016). The axial double probe and fields signal processing for the MMS mission. Space Science Reviews, 199(1–4), 167–188.

Le Contel, O., Leroy, P., Roux, A., Coillot, C., Alison, D., & Bouabdellah, A. (2016). The search-coil magnetometer for mms. Space Science Reviews, 199(1–4), 257–282.

Lindqvist, P.-A., Olsson, G., Torbert, R., King, B., Granoff, M., & Rau, D. (2016). The spin-plane double probe electric field instrument for mms. Space Science Reviews, 199(1–4), 137–165.

Pollock, C., Moore, T., Jacques, A., Burch, J., Gliese, U., & Saito, Y. (2016). Fast plasma investigation for magnetospheric multiscale. Space Science Reviews, 199(1–4), 331–406.

Russell, C., Anderson, B., Baumjohann, W., Bromund, K., Dearborn, D., & Fischer, D. (2016). The magnetospheric multiscale magnetometers. Space Science Reviews, 199(1–4), 189–256.